The relationship between thermal, rheological, and tack properties of copolyester-based hot melt adhesives

Michał Misiak, Paulina Latko-Durałek, Maria Mercedes Fernandez, Jorge L. Olmedo-Martínez, Dorota Kołbuk, Żaneta Górecka, Amir Malmir, Paulina Kozera, Alejandro J. Müller, Savvas G. Hatzikiriakos & Anna Boczkowska

Published online: 19 May 2025.

Submit your article to this journal

Article views: 127

View related articles

View Crossmark data

Taylor & Francis
Taylor & Francis Group

The relationship between thermal, rheological, and tack properties of copolyester-based hot melt adhesives

Michał Misiak[a] , Paulina Latko-Durałek[a,b] , Maria Mercedes Fernandez[c] , Jorge L. Olmedo-Martínez[c] , Dorota Kołbuk[d] , Żaneta Górecka[a] , Amir Malmir[e] , Paulina Kozera[a] , Alejandro J. Müller[c,f] , Savvas G. Hatzikiriakos[e] and Anna Boczkowska[a]

[a]Faculty of Materials Science and Engineering, Warsaw University of Technology, Warsaw, Poland; [b]Technology Partners Foundation, Warsaw, Poland; [c]POLYMAT and Department of Polymers and Advanced Materials: Physics, Chemistry and Technology, Faculty of Chemistry, University of the Basque Country, Donostia-San Sebastián, Spain; [d]Institute of Fundamental Technological Research, Polish Academy of Sciences, Warsaw, Poland; [e]Department of Chemical and Biological Engineering, University of British Columbia, Vancouver, BC, Canada; [f]Ikerbasque, Basque Foundation for Science, Bilbao, Spain

ABSTRACT

This paper studies the interrelationships between the molecular weight, rheology, crystallinity, and tackiness of three types of commercial thermoplastic hot melt adhesives. The hot melt adhesives employed here differ in their compositions and molecular weights, even though all are copolyesters primarily based on poly(butylene terephthalate). Differences in the composition were found to influence the adhesives' crystallization and melting behavior. These structural variations can translate into different thermal responses and processing characteristics relevant for tailoring adhesive selection to application requirements. Furthermore, adhesives with higher molecular weight were observed to possess larger elasticity, leading to significantly enhanced tackiness properties, as evidenced by the higher values of tensile modulus, peak stress, and work of debonding. This elevated tackiness was linked to the increased fibrillation process observed in polymers with higher molecular weights. Additionally, all tested adhesives exhibited storage moduli below the Dahlquist threshold ($G' < 3.3 \times 10^5$ Pa), which supports their ability to achieve measurable tackiness during the initial bonding process. The results presented in this study underscore the diversity among hot melt adhesives and the critical properties that should be considered when selecting adhesives for specific applications.

Introduction

Hot melt adhesives (HMAs) are a specific group of thermoplastic polymers that create an adhesive bond when heated, transitioning to a viscous-flow state. Upon subsequent cooling, they revert to their original physical state, thereby increasing their internal strength to ensure the structural integrity of the adhesive joint.[1] In contrast to liquid adhesives, they offer numerous advantages compared to traditional water- and solvent-based adhesives, such as robust mechanical strength without special substrate preparation, exceptional impact resistance, and high flexibility. Moreover, they present various benefits, including simplified processing and easier application

owing to their solid form, reduced health and environmental risks due to lack of harmful solvents, chemical resistance, and cost-effectiveness.[2,3] Hence, they are widely used as alternatives for the typical liquid adhesives in many industries, including packaging,[4] textiles,[5] building and construction,[6] automotive,[7,8] and electronics.[9,10]

Compared to standard homopolymers, HMAs have a more complex composition. They consist of several key components, including polymer bases, plasticizers, antioxidants, waxes, tackifiers, adhesion enhancers, and solid fillers. One of the base constituents in HMAs is usually a high molecular weight polymer, mainly responsible for its mechanical properties. The most widely used are ethylene-vinyl acetate copolymers, polyolefins, polyamides, copolyamides, and copolyesters.[11] Plasticizers increase the flexibility of the adhesive and reduce the viscosity of melted material, making it easier to apply. These can include low molecular weight polymers, dioctyl sebacate, oils, phthalates, or other compounds that improve the flexibility and workability of the adhesive.[12,13] Tackifiers and adhesion enhancers, although sometimes functionally overlapping, serve different purposes: tackifiers improve tack and melt flow, whereas adhesion enhancers promote interfacial bonding with low-energy surfaces. Common tackifiers include resins and their derivatives, as well as terpene and hydrocarbon resins.[14] It could also be silanes,[15] functionalized polymers, or other chemical substances that can create a better bond between the adhesive and the substrate. Waxes affect melting temperature, increase the open time (the working time before the adhesive cools and sets), and control the setting speed of the adhesive.[16] Antioxidants are added to prevent the oxidation and degradation of the adhesive, which can be exposed to heat, light, or oxygen. While they typically make up a tiny portion of the adhesive, usually less than 1 wt%, they are crucial for maintaining its performance and shelf life.[17] Solid fillers modify and improve the properties of the adhesive. For example, carbon fillers can impart electrical or thermal conductivity properties.[18] On the other hand, fillers such as wood flour, talc, magnesium oxides, or bentonite reduce material shrinkage, improve heat resistance, or lower production costs.[19]

The HMAs market exceeded $12.5 billion in 2022 and is expected to register a compound annual growth rate (CAGR) of 7.5% from 2023 to 2032. The anticipated market expansion can be attributed to the growing use of HMAs in various industries, including medical, packaging, automotive, electronics, and footwear.[20] Moreover, HMAs have also been utilized in the composites industry to enhance the bonding strength of hybrid parts,[21] improve the interlaminar toughness in lightweight composites,[18] and increase the adhesion between the nanofibrous mat and its supporting woven polyester fabric.[22] The newest application uses the HMAs as a matrix for the electrically conductive fillers, which could be used to enhance electrical conductivity of the fiber reinforced polymers as reported in the literature.[3,18]

Due to the growing interest in HMAs, much research has been dedicated to understanding their behavior and developing new formulations. Chu et al.[23] analyzed the influence of tackifier and wax content on the performance of ethylene-vinyl acetate-based HMAs, establishing correlations between these components and the material's rheological and peel strength properties. Their work highlighted the significance of compositional balance in optimizing adhesive properties. Similarly, Ignatenko et al.[14] evaluated HMAs based on styrene-isoprene-styrene rubber, focusing on rheological, mechanical, and adhesive properties compared to hydrocarbon resin-based formulations. Karakaya et al.[24] extended this understanding by examining the role of polymer type and adhesive layer thickness on the performance of adhesive joints, while Sandoval et al.[25] investigated how the microstructure and rheological properties of PBS-ran-PCL copolyesters influence their tack performance. However, these studies predominantly focus on controlled, lab-synthesized formulations, leaving a knowledge gap regarding commercially available HMAs having more complex compositions.

Building on the discussion above, this paper investigated the fundamental properties of three commercially available HMAs based on copolyester. The primary objective was to analyze how thermal and rheological properties influenced the tack behavior of the studied HMAs and to correlate these effects with their molecular weight. Given the limited research on commercially

available HMAs – particularly on their structure-property relationships in real-world applications – this study offers novel insights for practical use.

Materials and methods

Materials

Three commercially available HMAs based on copolyesters supplied by EMS-Griltech AG (Switzerland) with trade names: Griltex®2132, Griltex®1765, and Griltex®1839 were used as the test materials. Table 1 shows their properties included in the technical data sheets provided by the producer. All HMAs were in the form of pellets with a milky-like color. Pellets were dried in a vacuum oven at 40 °C for 12 h before further testing. The rheological and thermomechanical test specimens were prepared directly from the pellets by injection molding using a HAAKE MiniJet Piston Injection Molding System (ThermoFisher Scientific, Massachusetts, USA). The properties of each copolyester are listed in Table 1. Table 2 lists the conditions used in the injection molding process to prepare specimens for testing.

Chemical composition

Fourier transform infrared spectroscopy (FTIR) was used to identify the composition of each HMA. Samples for the analysis were fabricated using the injection molding method described in Section "Materials." FTIR spectra were collected using a Thermo Scientific Nicolet 6700 spectrometer with the attenuated total reflectance (ATR) technique. Each sample was scanned 64 times with a resolution of $4\,cm^{-1}$ in the frequency range $4000–400\,cm^{-1}$.

Molecular weight measurement

The molecular weight of the polymeric phase of the studied HMAs was assessed by gel permeation chromatography (GPC). The aliquots were prepared by dissolving materials in HFIP (1,1,1,3,3,3-hexafluoro-2-propanol, purity min. 99%) at a concentration of 20 mg/mL. Since the utilized system works with chloroform-filled columns, the obtained solutions were mixed with HPLC-grade chloroform (POCH S.A., Poland) to obtain 2 mg/mL solutions. After 24 h, filtration by PTFE membrane with a pore size of 0.22 μm was performed. The obtained clear polymer solutions were used in an autosampler attached to the GPC equipment. Aliquots of 100 μL were injected into the system and separated on two linear coupled SEC columns (PLgel 5 mm MIXED-C, UK, 300 × 7.5 mm) at 35 °C and a 0.7 mL/min flow rate. The molecular weight of the

Table 1. Properties of studied HMAs taken from the Technical Data Sheet (TDS).

Designation	Trade name	Melting point temperature (°C)	Melt volume rate (cm³/10 min) (160 °C/2.16 kg)	Melt viscosity [Pa·s] (160 °C/2.16 kg)
COPE_A	Griltex®2132	125	37	290
COPE_B	Griltex®1765	144	130	80
COPE_C	Griltex®1839	138–148	175	60

Table 2. Conditions used in the injection molding process to prepare specimens for testing.

Copolyester	Cylinder temp. (°C)	Mold temp. (°C)	Injection pressure (bars)	Injection time (sec)	Post processing injection pressure (bars)	Post processing injection time (sec)
COPE_A	132	35	900	2	800	2
COPE_B	150	35	700	2	650	2
COPE_C	170	40	500	2	300	1

samples was measured using a refractive index detector (Agilent, Singapore). The system was calibrated using nine polystyrene standards (Agilent, UK) with known molecular weights (M_p – peak molecular weight – ranging from 580 g/mol to 990,500 g/mol) and dissolved in the same mixture of HFIP and chloroform.

Wide-angle X-ray scattering

Wide-angle X-ray scattering (WAXS) was utilized to investigate the supermolecular structure of the studied HMAs. The measurements were performed using a Bruker D8 Discover diffractometer equipped with CuKα radiation at 40 kV and 40 mA. A reflection mode setup with Goebel optics was employed, featuring a 0.6 mm slit and a Soller collimator to optimize beam quality. A LynxEye 1-D silicon strip detector provided high sensitivity, enabling precise data acquisition over a diffraction angle range (2θ) of 5–35°. Background signals were subtracted using default instrument functions, and numerical deconvolution of WAXS profiles was conducted using PeakFit software. Crystalline diffraction peaks were modeled with Pearson VII functions, while the amorphous halo was represented by Gaussian profiles. The degree of crystallinity was computed as the ratio of the crystalline peak area to the total profile area.

Thermal properties

Differential scanning calorimetry (DSC) was used to determine calorimetric properties related to the materials' phase transitions. The pellets of HMAs were tested using a DSC Q1000 (TA Instruments, New Castle, USA) calorimeter according to ASTM D3418. For all materials, a heat-cool-heat cycle was applied in the temperature range from −80 °C to 200 °C in a nitrogen atmosphere. One constant heating rate (10 °C/min.) and four variable cooling rates (1 °C, 5 °C, 10 °C, and 20 °C/min.) were applied. The first heating run was carried out to obtain good sample contact with the pan, leading to a suitable heat flow and eliminating possible thermal history. The melting temperature (T_m), crystallization temperature (T_c), crystallization enthalpy (ΔH_c), and melting enthalpy (ΔH_m) were determined from the second heating. Due to the lack of literature data on the melting enthalpy for 100% crystalline copolyesters, their crystallinity content could not be calculated.

Rheological properties

Rheology measurements were performed on an Anton Paar parallel-plate geometry on injection-molded round specimens with a diameter of 25 mm and a thickness of 1.5 mm. First, a time sweep test was performed at 3 temperatures, similar to those used for the tack properties: 140 °C, 160 °C, and 180 °C with 1% strain (within the viscoelastic linear range) and a constant frequency of 10 rad/s. Consequently, the frequency sweep test was conducted at the same temperatures with a strain between 1% and 10% (within the linear viscoelastic range at the specific temperature) and with an angular frequency from 100 to 0.1 rad/s. All tests were conducted using the parallel-plate geometry and a gap of 1 mm.

Tack properties

The materials' tackiness properties were determined using an ARES strain-controlled rheometer (TA Instrument, New Castle, USA) equipped with parallel plates with an 8 mm diameter. About 25 mg of unmolten pellets was placed on the bottom plate, and once melted at $T = T_m$ + 10 °C, a layer of material with a thickness of 500 μm was formed. After 10 min, the temperature of the sample was lowered to 160 or 140 °C (depending on the material), and the probe tack test was carried out in three stages: (1) compression, where the top plate was

lowered at a constant speed of 0.1 mm/s, reaching a fixed distance from the lower plate of h_0 = 50 μm; (2) contact period for 60 s; and (3) debonding (plate separation) at speed (V_{deb}): 0.314 mm/s. The same test was also conducted at $T = 180\,°C$ with three repetitions for each studied HMAs. Data of force (F) and displacement ($h(t)$) were collected during each experiment and subsequently converted into stress (σ) and strain (ε) curves using Equations (1)–(3):

$$\sigma = \frac{F}{A_{max}} \tag{1}$$

$$\varepsilon = \frac{h(t) - h_0}{h_0} \tag{2}$$

$$\frac{d\varepsilon}{dt} = \dot{\varepsilon} = \frac{V_{deb}}{h_0} \tag{3}$$

where A_{max} is the contact area between the probe and the material during the compression stage, h_0 is the initial layer thickness, $h(t)$ is the adhesive thickness as a function of time, and $d\varepsilon / dt$ represents the linear strain rate.

The following characteristic properties can be determined from these stress-strain curves illustrated in Figure 1: (a) the tensile modulus E, within the linear regime (low strains or short times), (b) the peak stress, σ_{max}, (c) the maximum extension ε_{max}, and (d) the work of debonding or adhesion W_{deb}, which is the area under the loading curve multiplied by the initial layer thickness h_0, as indicated by Equation (4):

$$W_{deb} = h_0 \int_0^{\varepsilon_{max}} \sigma(\varepsilon) d\varepsilon \tag{4}$$
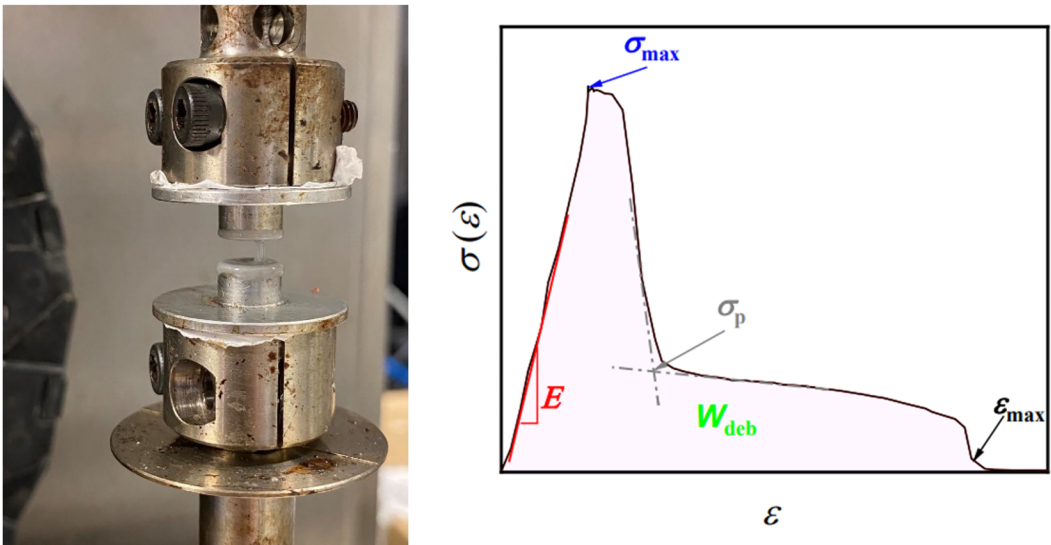
Figure 1. Schematic stress–strain curve obtained during probe-tack experiments. Reprinted with permission from reference[25] (CC BY licensed, Copyright (c) 2022).

Results and discussion

Chemical composition

FTIR was used to compare the chemical composition of the three HMAs studied. Using this method, it was not possible to establish the full composition of the materials due to the presence of a few unknown components. However, according to Figure 2, the selected HMAs are based on the same type of polymer because their spectra are nearly identical. Each copolyester exhibited a strong band at $1710\,cm^{-1}$ corresponding to the carbonyl group (C=O) stretching vibration characteristic of esters. Bands in the $1260–1240\,cm^{-1}$ range and a strong peak at $1100\,cm^{-1}$ come from the vibration of ester groups. A sharp band at $725\,cm^{-1}$ corresponds to the vibration of C–H out-of-plane in an aromatic ring, while a broad peak at $2925–2853\,cm^{-1}$ refers to the –CH_2– symmetric and asymmetric stretch.[26,27] Based on the spectra analysis and with the help of the software library, the studied copolyesters contain polybutylene terephthalate (PBT) as the main polymer. The same type of polymer was determined by WAXS analysis (see Section "Crystallinity").

Compared to COPE_A and COPE_C, the spectrum of COPE_B shows distinct features in the regions of $1200–1300\,cm^{-1}$ and $2900–3000\,cm^{-1}$. The variation in the $1200–1300\,cm^{-1}$ region may be attributed to subtle differences in the C–O stretching vibrations, potentially reflecting the presence of different comonomers or copolyester architectures. In the $2900–3000\,cm^{-1}$ range, the slight shift and intensity change in the C–H stretching region could indicate differences in aliphatic chain content or the presence of plasticizers or other additives.

Molecular weight

The results of the GPC analysis are presented in Figure 3 and in Table 3. The studied HMAs have different molecular weight distributions expressed by the number average molecular weight (M_n), weight average molecular weight (M_w), and polydispersity index, *PID* (see Table 3). The highest M_n and M_w were observed for COPE_A, 8.15 kDa and 50.5 kDa, respectively, whereas the lowest M_n and M_w were observed for COPE_C, 5.17 kDa and 25.2 kDa, respectively. For
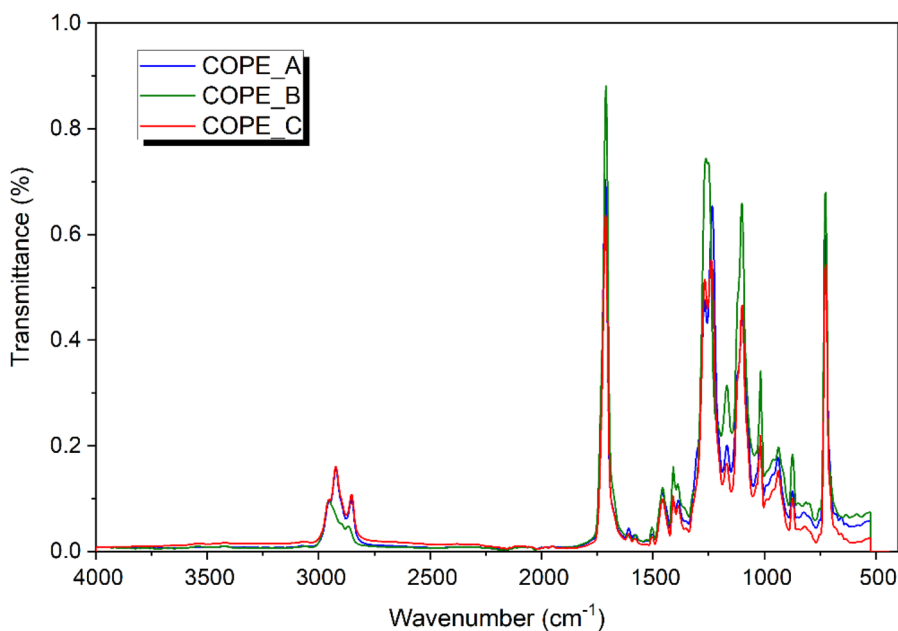
Figure 2. The comparison of FTIR spectra of studied HMAs.

COPE_B, the M_n was 8.82 kDa and the M_w was 37.3 kDa. The polydispersity index revealed the widest molecular weight distribution for COPE_A and the narrowest for COPE_B. These differences come from the specific composition of each HMA, which, despite their nearly identical FTIR spectra shown in Figure 2, are different as far as their composition is concerned.

Crystallinity

The WAXS spectra confirm that the main component in the tested HMAs is a PBT copolyester, which is consistent with FTIR analysis. In general, PBT might exhibit triclinic crystalline polymorphism with α and β forms and a smectic liquid crystalline phase, transitions between these forms depending on processing conditions such as applied stress or temperature.[28] Analyzed copolyesters exhibited characteristic diffraction peaks at 2θ angles of c.a. 9°, 15°, 17°, 20°, 23°, and 25.1°, corresponding to the (001), (011), (010), (110), (100), and (111) planes of the stable α-crystalline form (Figure 4(a), Table 4). These peaks indicate well-ordered structures, with the (010) and (100) planes aligned parallel to the polymer chain axis and the (001) plane perpendicular. An example of the WAXS spectra fitting is illustrated in Figure 4(b). Quantitative analysis revealed a crystallinity range of 44–67%, with much higher crystallinity found for COPE_A. These differences are probably influenced by various additives that could be present in these HMAs (Table 4). The sharper and more intense XRD peaks observed for COPE_A, which indicate a higher degree of crystallinity, are consistent with FTIR results showing more defined ester and carbonyl absorption bands, suggesting a more regular and ordered copolyester structure. Conversely, the broader peaks for COPE_B and COPE_C in both FTIR and XRD indicate lower ordering and potentially a higher proportion of amorphous regions. These findings corroborate earlier studies indicating α phase, without β and smectic phases observed in high-speed spun fiber.[29]
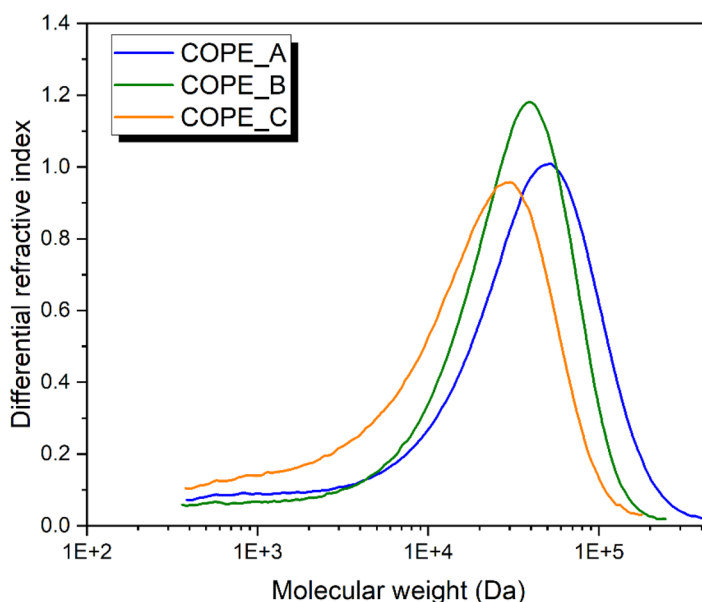
Figure 3. The molecular weight distributions of the three tested copolyester HMAs.

Table 3. Molecular weight characteristics of the three tested HMAs.

	M_n (Da)	M_w (Da)	PID
COPE_A	$8.15 \cdot 10^3$	$5.05 \cdot 10^3$	6.2
COPE_B	$8.82 \cdot 10^3$	$3.73 \cdot 10^3$	4.2
COPE_C	$5.17 \cdot 10^3$	$2.52 \cdot 10^3$	4.9
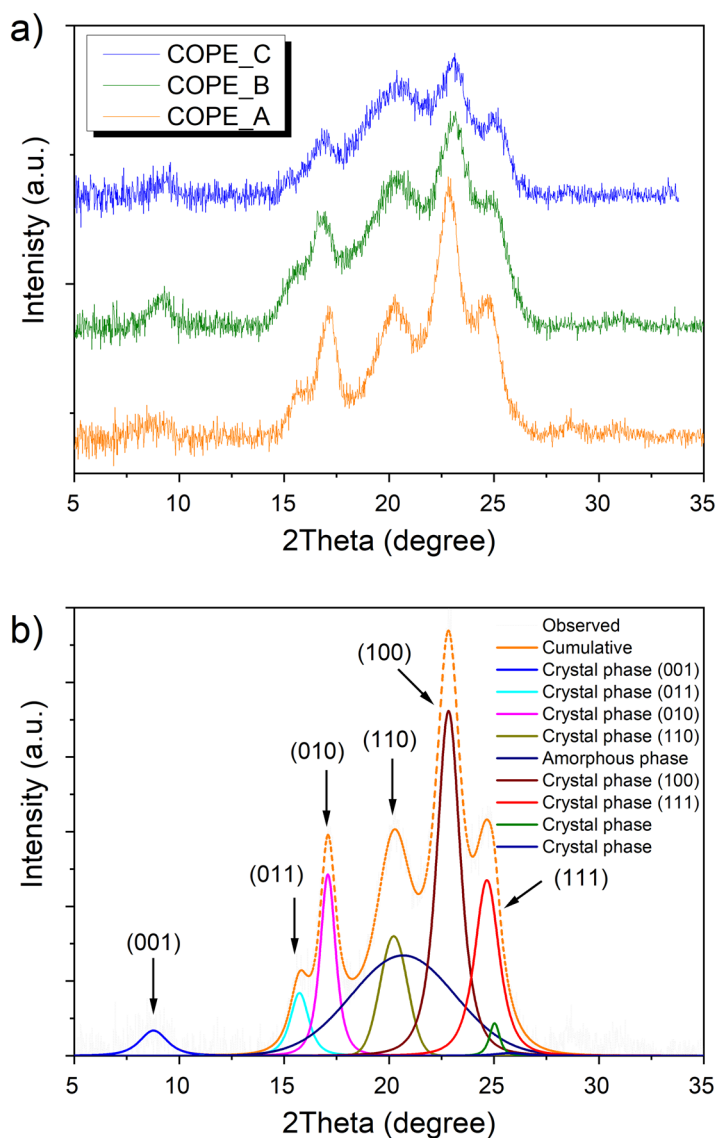
Figure 4. (a) Wide angle X-ray scattering (WAXS) spectra of analyzed samples and (b) fitting of WAXS spectra of COPE_B.

Table 4. Crystallinity and the main diffraction peaks at 2θ Braggs angles, corresponding to the diffraction planes of (001), (011), (010), (110), (100), and (111) of analyzed materials.

	COPE_A	COPE_B	COPE_C
Crystallinity (%)	69	44	48
2Θ of (001) (°)	9	9	9
2Θ of (011) (°)	16	16	15
2Θ of (010) (°)	17	17	17
2Θ of (110) (°)	21	201	20
2Θ of (100) (°)	23	23	23
2Θ of (111) (°)	25	25	25

Calorimetric properties

The results of the DSC analysis are presented in Figure 5 and summarized in Table 5. Figure 5(a,c,e) illustrates the DSC cooling traces at varying cooling rates of 1, 5, 10, and 20 °C/min, while Figure 5(b,d,f) shows the corresponding second heating curves for COPE_A, COPE_B, and COPE_C, respectively.

The DSC cooling scans reveal distinct differences in the crystallization behavior of the three copolyesters. COPE_A does not exhibit crystallization exotherms during cooling, even at the lowest cooling rate of 1 °C/min. This suggests restricted chain mobility, which could be caused by high molecular weight and dispersity index. Upon subsequent heating, COPE_A undergoes a glass transition at −12.7 °C at 1 °C/min cooling rate, followed by a cold crystallization exotherm at around 51.8–54.5 °C and a broad melting peak between 112 °C and 122 °C. The comparable values of cold crystallization enthalpy (ΔH_{cc}) and melting enthalpy (ΔH_m) suggest that most of the crystallization occurs during heating, consistent with the presence of rigid amorphous fractions affecting crystallization kinetics in PBT-based systems as described in prior studies.[30,31] According to WAXS analysis, COPE_A exhibits the highest crystallinity (69%) among all analyzed HMA. The diffraction peaks at characteristic 2θ angles for the α-crystalline phase of PBT
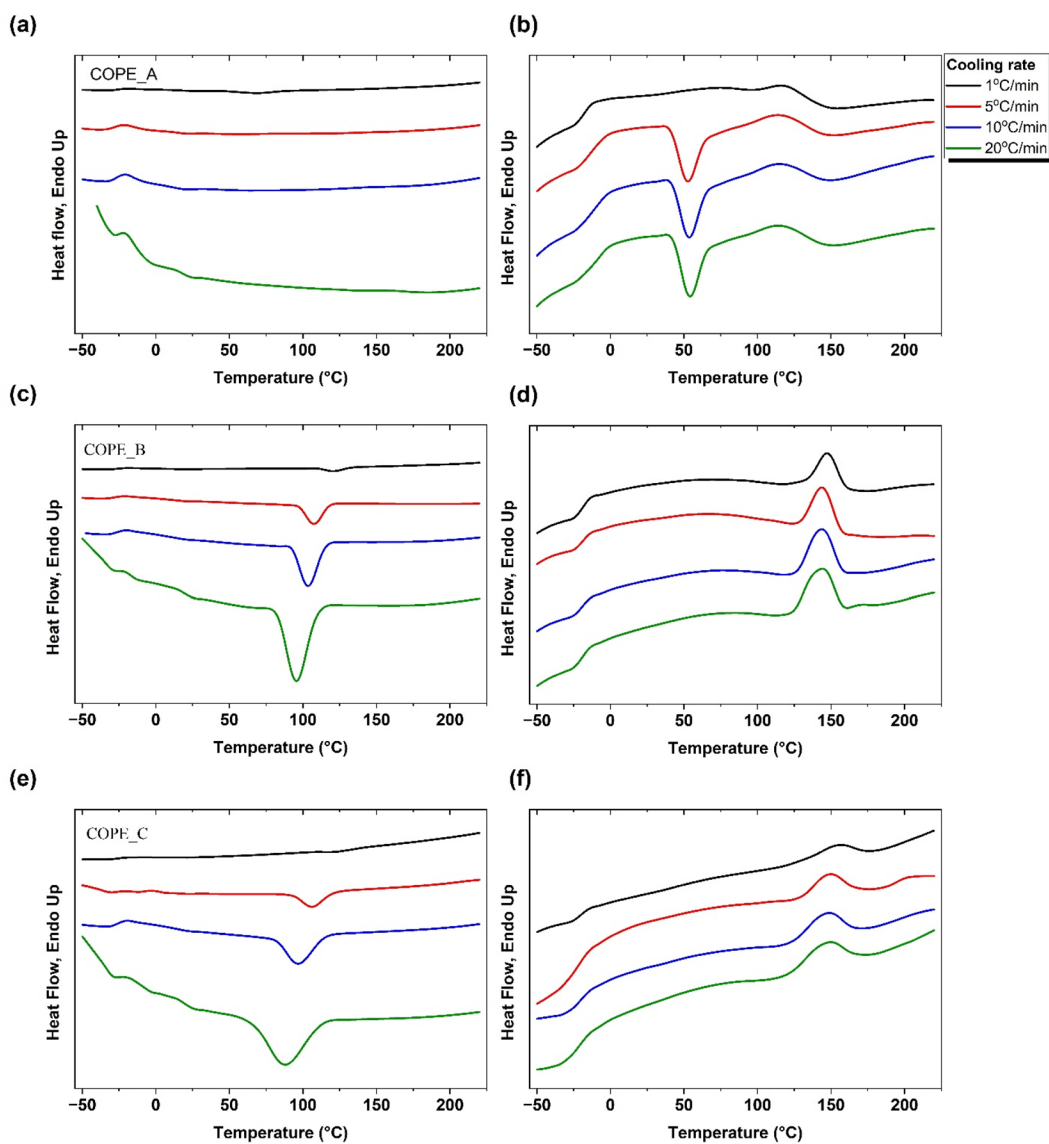
Figure 5. (a) DSC cooling scans of COPE_A; (b) second DSC heating scans of COPE_A; (c) DSC cooling scans of COPE_B, (d) second DSC heating scans of COPE_B, (e) DSC cooling scans of COPE_C, (f) second DSC heating scans of COPE_C. Four different cooling rates were applied and one constant heating rate (10 °C/min.).

Table 5. The determined DSC parameters of three tested HMA at four different cooling rates.

	Cooling		Second heating				
	T_c (°C)	ΔH_c (J/g)	T_g (°C)	T_{cc} (°C)	ΔH_{cc} (J/g)	T_m (°C)	ΔH_m (J/g)
COPE_A							
1 °C/min	–	–	−12.7	–	–	122.4	5.6
5 °C/min	–	–	−10.5	51.8	9.2	115.4	9.7
10 °C/min	–	–	−9.3	54.5	11.1	112.3	10.9
20 °C/min	–	–	−8.0	54.2	12.2	113.7	11.8
COPE_B							
1 °C/min	120.2	17.4	−19.1	–	–	149.4	9.8
5 °C/min	106.4	19.4	−19,3	–	–	145.9	11.5
10 °C/min	103.3	21.8	−19.2	–	–	145.5	13.9
20 °C/min	95.4	23.9	−19.3	–	–	146.6	13.3
COPE_C							
1 °C/min	122.3	15.4	−20.9	–	–	154.5	6.4
5 °C/min	105.0	15.6	−20.1	–	–	149.6	7.4
10 °C/min	95.6	19.3	−19.6	–	–	144.2	9.7
20 °C/min	85.6	23.8	−19.4	–	–	148.1	11.1

confirm the presence of ordered crystalline domains formed during cooling after injection molding, consistent with the high crystallinity observed in the DSC analysis.

In contrast, COPE_B and COPE_C exhibit well-defined crystallization exotherms during cooling, with crystallization temperatures (T_c) decreasing as the cooling rate increases. For example, COPE_B crystallizes at T_c = 120.2 °C at 1 °C/min and at T_c = 95.4 °C at 20 °C/min. Similarly, COPE_C shows T_c values decreasing from 122.3 °C to 85.6 °C with increasing cooling rates. The second heating curves reveal minimal cold crystallization and broad melting peaks at approximately 145–154 °C. These broad peaks may reflect recrystallization processes during heating. The WAXS results corroborate these observations by confirming lower crystallinity values for COPE_B (44%) and COPE_C (48%) compared to COPE_A. The diffraction patterns for COPE_B and COPE_C are consistent with the broader melting transitions observed in the DSC scans. This difference in melting behavior also suggests variations in the distribution of lamellar thickness among the tested materials. COPE_B and COPE_C, which crystallized during cooling, exhibited narrower and more symmetric melting peaks, indicative of a more uniform lamellar thickness and a higher degree of crystalline order. In contrast, COPE_A, which did not crystallize during cooling and underwent cold crystallization during heating, showed a broader melting peak. Such broad peaks are typically associated with a wider lamellar thickness distribution, resulting from less organized and less thermally stable crystalline structures formed during heating.[32] These observations are in line with prior studies showing that cold crystallization often leads to imperfect or thinner lamellae due to limited chain mobility and delayed nucleation.[33]

The combined DSC data underline the three copolyesters' distinct thermal and structural behavior, which can be attributed to differences in molecular weight and compositional variability. For instance, the presence and distribution of non-crystallizable comonomer units within the copolymers could affect the crystallization kinetics and thermal stability. COPE_A's slower crystallization kinetics and higher crystallinity suggest it forms highly stable crystalline domains during heating, making it suitable for higher thermal stability applications. In contrast, COPE_B and COPE_C exhibit faster crystallization and broader melting transitions, indicating greater flexibility and suitability for processing at varied cooling rates.

Rheological properties

The results of the oscillatory time sweep test for the three studied HMAs are presented in Figure 6. During this test, the material changes over time at the specific temperature are monitored, here at 140 °C for COPE_A and at 160 °C for COPE_B and COPE_C (Figure 6(a)); and at 180 °C
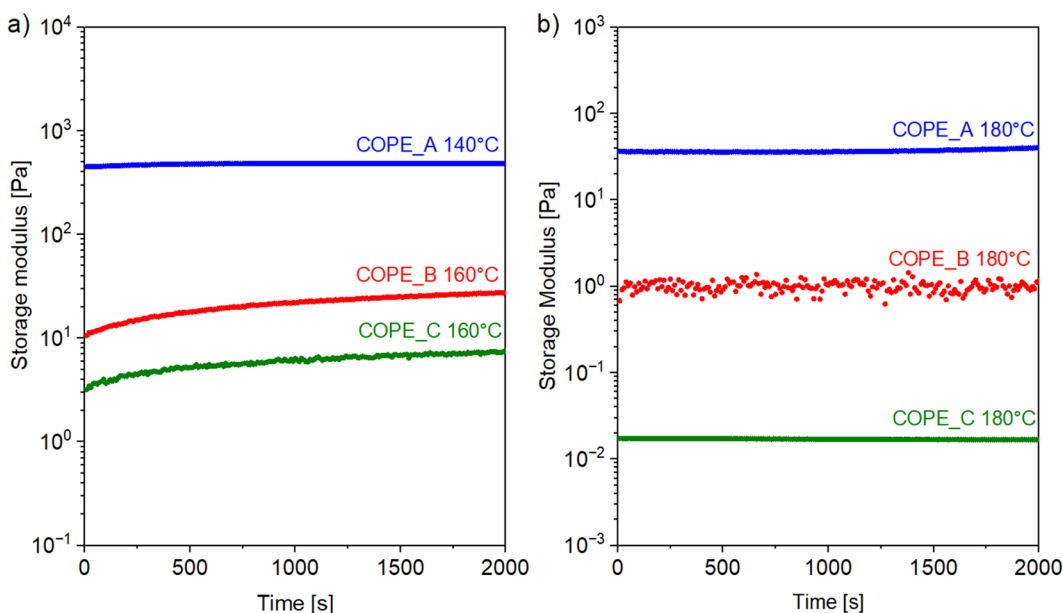
Figure 6. The changes in the storage modulus of copolyesters over the time at different temperatures.

for all COPEs (Figure 6(b)). These temperatures are the same as those used in the tack test. The graphs show that COPE_A is stable at 140 °C and 180 °C over 33 min. Similarly, COPE_C is stable within the measuring time at 160 °C and at 180 °C. In the case of COPE_B, the storage modulus is stable at lower temperature; however, at 180 °C slight, variations are easily noticed over the whole testing period. This is possibly related to the structure rearrangements at that temperature due to the much lower viscosity of COPE_B compared to those of COPE_A and COPE_C. In addition, additives could influence melt stability by locally affecting the viscosity and chain mobility of the tested materials.

Figure 7 presents frequency sweep test results for the studied HMAs. All copolyesters behave like a Newtonian liquids with viscoelastic moduli independent of frequency (Figure 7(a)). The highest viscosity is possessed by COPE_A (highest molecular weight), followed by COPE_B and COPE_C. These are consistent with their molecular weight listed in Table 3. At lower temperatures, the viscosity is higher than at 180 °C, which is related to increased relaxation times at lower temperatures. To explain the tackiness properties (Section "Tack Properties") of the copolyesters, their elastic moduli are plotted in Figure 7(b). The graph shows that COPE_A shows a significantly higher elastic modulus at both temperatures compared to those of COPE_B and COPE_C. Therefore, COPE_A should possess the highest adhesion properties expressed by the tackiness indicators (σ_{max} and W_{deb}). According to the Dahlquist criterion, the materials with a dynamic shear modulus (stiffness) of less than 10^5 Pa when deformed in 1 s will exhibit "tack". When the application requires tack to develop either faster or slower than in a typical finger pressure test, the criterion will be shifted – to higher stiffness values for longer dwell times and lower values for shorter ones or rougher surfaces.[30] In summary, a material with good adhesion properties should meet the assumption of $|G'| < 3.3 \cdot 10^5$ Pa. The Dahlquist criterion is fulfilled by all tested materials, as shown in Figure 7. Therefore, at the temperatures studied and at all experimental frequencies, the polymeric chains are able to relax on a long time scale, as indicated by the predominantly viscous behavior, G'<G". This flow regime is governed by the molecular structure of the chains and is very sensitive to molecular weight and polydispersity effects. In addition, it is interesting to note that there is some deviation from the terminal behavior in the low-frequency range, which significantly broadens the distributions of the relaxation times, providing some elastic character even at low strain rates. In the following section, we will discuss the effect of the
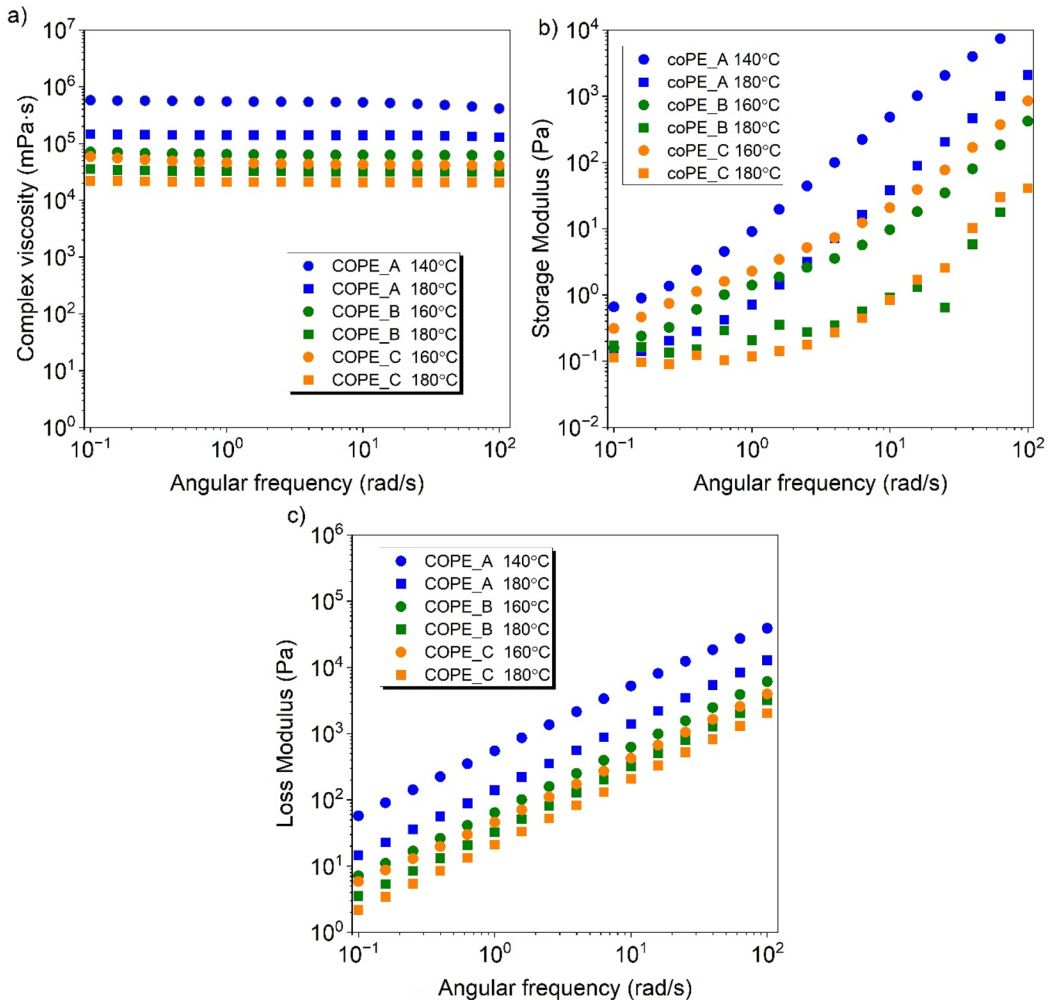
Figure 7. (a) Complex viscosity and (b) storage modulus of the copolyesters (c) loss modulus at 140 °C, 160 °C, and 180 °C.

different rheological contribution to the immediate adhesiveness or tack response, which is relevant not only to establishing the quality control of these adhesives, but also to contributing to the understanding of the mechanism of adhesion and its relationship with the molecular structure.

Tack properties

Tackiness or adhesion is the property of an adhesive that enables it to form a bond of measurable strength after coming into contact with a substrate under short time and light pressure. An ideal adhesive should possess sufficient tack to bond effectively to the specific surface and exhibit resistance to detachment.[31] That is, both liquid properties to wet the surface when the bond is formed and solid properties to sustain a certain level of stress during the process of debonding are necessary. Therefore, tack properties have traditionally been correlated to the linear viscoelastic properties, such as elastic and loss modulus. However, the tackiness is a complex and not yet completely understood mechanism. As established by microscopic approaches,[34,35] the deformations occurring during the tack experiment involve large and transient behaviors that cannot be easily predicted by either viscosity (shear, elongational) or any other small strain steady-state dynamical property. Therefore, it is relatively difficult to establish simple

criteria for a good adhesive material, as the tackiness is dependent on several factors concerning the properties of the adhesive (composition, molecular weight, viscoelastic properties) and the type of adherent, temperature, pressure, and contact time.[36]

Despite the difficulties in linking adhesion parameters to linear viscoelastic results, we have tried to discuss experimental correlations between the most significant parameters of Figures 1 and 7 and the melt elasticity reported in Section "Rheological properties." For this purpose, we rely on previous experimental and theoretical studies based on the widely studied mechanics of the probe adhesion test. The shape of the stress-strain curve obtained during the detachment of the probe from the adhesive film is well established to characterize the adhesive performance of the tested material and depends on the rheological properties of the adhesive layer and on the interfacial interactions between the adhesive and the substrate.[37] Typical characteristic values extracted from the curve are the maximum tensile stress, σ_{max}, the stress at the beginning of the plateau, σ_p, the maximum nominal strain to failure, ε_{max}, and the adhesion energy, W_{adh} (the integral under the stress-strain curve), as pictured in the schematic graph in Figure 1. These characteristic parameters correlate to the sequence of events developed during the test. It begins with the bonding of the adhesive film to the surface of the adherent established during the compression and contact stages, and then, it follows the debonding mechanism that implies (1) the formation of cavities or cracks at the interface or in the bulk, (2) the formation and elongation of a fibrillated structure, and (3) the detachment either by cohesive or adhesive failure of the fibrils from the probe surface.[36]

Hence, in this study we analyze the three HMAs that differ in their intrinsic properties (molecular weight, thermal, and rheological) at various temperatures. The results of the tack test are presented in Figure 8(a,b), while the determined characteristic parameters are listed in Table 6. These results contain information on the response of the adhesives at the different stages of the bonding – debonding probe tack test.

During the bonding process, the wetting ability of the adhesive to the substrate is related to the energy required to deform the adhesive and adapt it to the adherent surface. This first
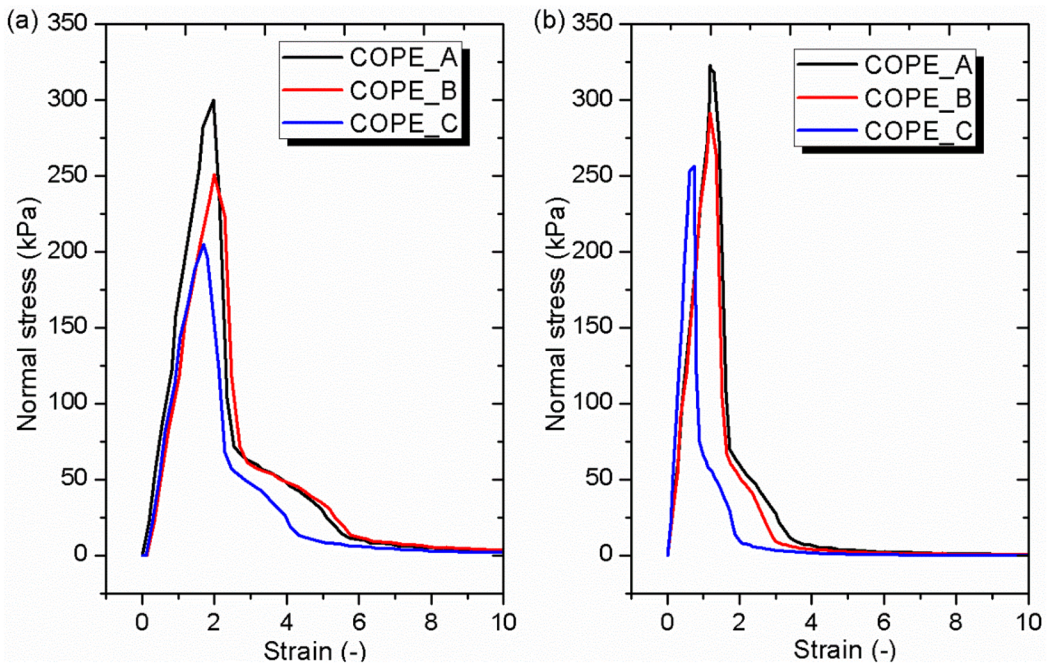
Figure 8. Stress-strain curves for tested hot melt adhesives at $T = T_m + 10\,°C$ (a) and at $T = 180\,°C$ (b). The test velocity was 0.314 mm/s.

Table 6. Characteristic parameters obtained from stress-strain curves at T_m+10 °C and 180 °C.

Hot melt adhesive	Test temperature (°C)	Characteristic parameters		
		E (kPa)	σ_{max} (kPa)	W_{deb} (J/m2)
COPE_A	140	166.8	300.1	29.1
	180	261.3	322.9	19.1
COPE_B	160	143.7	252.1	27.1
	180	252.4	291.4	16.2
COPE_C	160	137.7	204.8	19.2
	180	333.6	256.6	9.2

Test velocity V_{deb} 0.314 mm/sec.

requirement commonly uses the Dahlquist criterion to evaluate both hot melt and pressure-sensitive adhesives.

On the other hand, the mechanical analysis of the cavitation process during debonding tests predicts the growth of cavities after the cavitation starts for an applied hydrostatic tensile pressure exceeding the tensile modulus of the adhesive.[38] The measured σ_{max} is theoretically and experimentally confirmed to be related to the elastic modulus of the adhesive.[39] Lakrout et al.[35] reported that the σ_{max} at a given debonding rate is directly proportional to G' (the value of the elastic modulus measured with steady oscillatory shear measurements at an equivalent reduced average deformation rate). Confirming the findings of Lakrout et al.,[35] Creton and Ciccoti[40] established a strong correlation between the development or enlargement of cavities and the elastic properties of adhesives. They suggested that the growth of cavities implies small local elastic deformations involved in the debonding process. But the debonding process cannot be explained by a simple model for the nucleation of cavities. According to Chiche et al.,[41] the cavities may occur to expand from defects at the interface during the bonding process, the size and density of the initial defects at the bond interface also influencing σ_{max}. These considerations imply that, generally, provided the Dahlquist criterion is met, it will follow that the higher the modulus of the adhesive, the greater the bond strength on a high-energy surface. According to this statement, from the curves presented in Figure 8, it can be seen that the studied HMAs have different degrees of tackiness. From the results obtained at T_m+10 °C (Figure 7(a)), it can be concluded that COPE_A has the highest adhesive properties among the three tested materials, as indicated by its higher tensile modulus ($E = 166.8$ kPa), peak stress ($\sigma_{max} = 300.1$ kPa), and work of debonding ($W_{deb} = 29.1$ J/m²). The results suggest that COPE_A provides greater resistance to deformation, requires higher stress to reach its peak, and needs more energy to be debonded. COPE_B possesses lower adhesion properties compared to COPE_A, while COPE_C is characterized by the lowest tackiness.

The second stage of debonding, once the cavitation process occurs, is the formation of separated fibrils, as each cavity achieves a steady-state cross-sectional area.[35] Fibril's elongation occurs during the characteristic stress plateau, clearly observed for all the samples in Figure 8, in line with findings reported by Lakrout et al.,[35] who demonstrated the strong correlation between increased fibrillation and higher molecular weights in polymeric adhesives. The energy required to continue extending the fibrils will eventually exceed the adhesion between the adhesive and the plate, and failure will occur through cohesive fracture or by separation of the adhesive from the probe surface, as it well explained by O'Connor et al.[31] The peak of the shoulder, σ_p, and the elongation at break, ε_{max}, are the parameters related to the formation of fibrils and reflect the cohesive strength of the adhesive and the interfacial adhesion (for low molecular weights is expected that those values are close to zero because low molecular weights favor the quick coalescence of the cavities). Therefore, the different debonding and fibrillation behaviors are dependent on molecular weight. It is reported by Oconnor et al.[31] that for blends of model polyisobutylenes, only those blends with molecular weight of 850 kg/mol, or higher, show strong fibrillation. In this range, they observed that the elongation at break slightly decreased with increasing molecular weight, while the shoulder strongly

increased.[35] The stress-strain curves of the copolyesters in Figure 8 confirmed the presence of the fibrillation signature that makes the significant contribution to the work of adhesion expected for HMAs. During the tack test, the high molecular weight chains provided high resistance to the fiber stretching, increasing the area under the curve. Interestingly enough, the characteristic plateau region is similar for COPE_A and COPE_B, both with similar M_n values, while COPE_C, with a lower M_n value, showed the lower stress value in the plateau. Concerning the deformation at break, ε_{max}, it was observed that the strain maximum did not decrease with increasing the molecular weight; that is, ε_{max} for COPE_A and COPE_B was higher than ε_{max} for COPE_C. The results could be related to the polydispersity of these materials, since the presence of lower molecular weight chains would offer good fiber fluidity.

The adhesion work, calculated from the area under the stress-strain curves at the low temperatures, $T = T_m + 10°C$, in Figure 8(a), shows that the response is dominated both by the high value of the initial peak, a consequence of the good wetting of these adhesives, and by the ability to dissipate energy during the fibrillation and debonding process. However, the adhesion behavior obtained at the higher temperature, $T = 180°C$, showed a complex effect depending on the region of the stress-strain curve analyzed. The overall tack properties of the studied HMAs at 180°C (Figure 8(b)) showed the same dependence as those at $T_m + 10°C$, with the highest value of debonding energy exhibited by COPE_A and the lowest by COPE_C. For all materials, the tensile modulus and peak stress, σ_{max}, increased; nevertheless, the work of debonding decreased at a temperature 180°C. Such behavior may be due to the test temperature being too high, which indicates that this is a temperature outside the optimal window of use for these adhesives. It lowers the adhesive's mechanical strength, and a small amount of work is needed for debonding.

The temperature of the test is important because it modifies the polymer's relaxation times and therefore the material's rheological behavior. As expected, an increase in the temperature was observed to decrease the elastic modulus of copolyesters (Figure 6). Therefore, the measured σ_{max} peaks at $T = 180°C$ were expected to be lower than at $T = T_m + 10$, but the tack stress-strain curves, as mentioned before, showed opposite behavior (Figure 8(b)). As described previously, the process of debonding is rather complex and involves the nucleation of cavities, the growth of these cavities, and the formation of the fibrillar structure. Ideally, one would expect a time-temperature equivalence able to predict the tack behavior at different temperatures and debonding rates through similar trends rather than to predict the tack behavior at different temperatures and debonding rates through similar trends to the rheological properties. However, the value of σ_{max} not only depends on the adhesive's rheological properties but is also considered a function of the size and real density of the initial defects present at the interface between the adhesive and the flat substrate.[39] These initial defects are formed during the compressive contact stage, presumably by the trapping of submicron air bubbles. Therefore, the different scale of the temperature's effect on the defects' density and the elastic modulus would invalidate the time-temperature superposition. The complex thermal effect would effectively decrease the shear modulus as the temperature increases and decrease the defect density due to better contact, so the nucleation of cavities would occur for higher levels of average stress, accounting for a higher σ_{max}. Lindner et al.[42] reported a similar result for model pressure-sensitive acrylic adhesives. According to the authors, thermally induced changes during the cavitation mechanism would explain the time-temperature nonequivalence of the σ_{max} vs strain relationship. However, since the stress plateau parameter is considered to be unaffected by the contact mechanism, the σ_p vs. strain relationship would be time-temperature equivalent. Consequently, the effect of temperature on the fibrillation event of the copolyesters at $T = 180°C$ was as expected. A less pronounced fibrillation plateau was observed, although it did not disappear completely, so that after the initial peak, σ_p, there was a continuous decrease in stress with increasing strain, consistent with the loss of elasticity at the higher temperatures.

Adhesion is related to the molecular weight of the adhesives, which is the highest for COPE_A. According to literature, adhesion is enhanced with higher molecular weight of polymer, attributed to the presence of entanglements that facilitate the fibrillation process.[31,43] But adhesion is also

a temperature-dependent phenomenon, since the decrease in elasticity results in a decrease in the work of adhesion, as reported in the literature for different systems.[44] This behavior clearly reflects that the tackiness response depends on viscoelastic properties, understood as the balance between viscous flow and elastic deformation. Viscous flow (low viscosity, low elastic modulus) means that the adhesive response offers low resistance to deformation; excessive elasticity (high viscosity, high elastic modulus) implies that the adhesive may not make good contact with the substrate.[43] As mentioned in Section "Rheological properties," COPE_A showed the highest elastic modulus, followed by COPE_B and COPE_C, which were consistent with the determined adhesion properties.

Conclusions

This study characterized three commercial hot melt adhesives based on polybutylene terephthalate by their thermal, rheological, and tack properties. The results showed significant differences between the adhesives caused by variations in molecular weight and possible use of different aliphatic comonomers or additives, affecting molecular weight and crystallinity. COPE_A had the highest molecular weight and crystallinity, and COPE_C had the lowest molecular weight and viscosity of the three adhesives. The WAXS analysis confirmed that all adhesives exhibited the same α-crystalline phase of PBT, with minor differences in diffraction angles, likely resulting from structural imperfections caused by aliphatic comonomers. COPE_A has the highest crystallinity and formed thermodynamically stable crystalline domains during heating, while COPE_B and COPE_C had lower crystallinity. These results show how molecular weight and crystalline structure affect the thermal and mechanical properties of the adhesives.

Copolyesters with narrower molecular weight distributions, like COPE_B and COPE_C, showed melting behavior within a narrower range, meaning a more uniform lamellar thickness distribution. COPE_A did not crystallize during cooling at any of the cooling rates (1, 5, 10, and 20 °C/min) and showed cold crystallization and fusion during heating. This behavior was attributed to its higher molecular weight, which may hinder chain mobility and delay crystallization under non-isothermal conditions.

During the time sweep test at 140 °C, 160 °C, and 180 °C, all the HMAs showed thermal stability except COPE_B, which showed lower stability at higher temperatures. This could be due to its lower viscosity and a small degree of thermal degradation.

The study also showed the effect of the adhesives' molecular weight and rheological behavior on their tackiness. COPE_A showed the highest tackiness at lower and higher temperatures, as seen in higher values of tensile modulus, peak stress, and work of debonding. This higher tackiness was due to COPE_A's higher molecular weight distribution, whose higher degree of entanglement reinforced the fibrillation during debonding. COPE_C with lower molecular weight showed the lowest tack of the three adhesives.

To sum up, this study provides more insight into the factors that affect the performance of HMAs, important for their practical applications. The combination of thermal, rheological, and crystallinity analysis allows us to monitor the differences between HMAs and understand their tackiness and adhesion.

Disclosure statement

Funding

Notes on contributors

Below, we provide a detailed breakdown of responsibilities alongside an approximate percentage of each author's overall contribution in the publication "The Relationship Between Rheological, Thermal, and Tack Properties of Copolyester-Based Hot Melt Adhesives."

1. Michał Misiak (30%)
Conceptualization: Developed the overarching research goals and the initial concept of the study.
Methodology: Designed and described the experimental thermal analysis and tack property testing procedures.
Investigation: Performed the thermal and tack property experiments, collected data, and interpreted the results.
Data Curation: Organized and maintained all experimental datasets.
Formal Analysis: Analyzed experimental outcomes and drew conclusions.
Visualization: Prepared figures, tables, and other visual materials.
Writing – Original Draft: Composed the initial draft of the manuscript, including the introduction, conclusions, and article abstract.
Writing – Review & Editing: Provided overall editorial revisions and integrated feedback from coauthors.

2. Paulina Latko-Durałek (25%)

Conceptualization: Contributed to formulating the study concept, particularly for the rheological investigations.

Formal Analysis: Analyzed and interpreted the rheological data, drew conclusions, and elaborated correlations.

Funding Acquisition: Secured financial support for the research.

Writing – Original Draft: Contributed to drafting the initial manuscript framework.

Writing – Review & Editing: Revised and edited the manuscript for coherence, clarity, and style.

3. Maria Mercedes Fernandez (5%)

Investigation: Assisted in performing the tack property experiments.

Validation: Provided expertise in verifying the accuracy and reliability of the tack property data.

Writing – Review & Editing: Offered critical feedback on data interpretation and manuscript revisions.

4. Jorge L. Olmedo-Martinez (5%)

Investigation: Assisted in conducting DSC (Differential Scanning Calorimetry) experiments.

Methodology: Provided expert guidance on DSC procedures and analysis protocols.

Validation: Verified thermal analysis data and contributed to the accuracy of experimental results.

5. Dorota Kołbuk (6%)

Methodology: Developed and described the experimental methodology for WAXS (Wide-Angle X-ray Scattering).

Investigation: Performed WAXS measurements and collected relevant data.

Writing – Original Draft: Authored the methods section and participated in discussing WAXS results.

6. Żaneta Górecka (5%)

Methodology: Established and documented the procedures for measuring molecular weight of the hot melt adhesives.

Investigation: Carried out the molecular weight analyses.

Writing – Original Draft: Drafted the relevant methodology and contributed to the discussion of results.

7. Amir Malmir (5%)

Investigation: Conducted rheological testing of the copolyester-based adhesives.

Formal Analysis: Provided insights and participated in the discussion of the rheological data.

8. Paulina Kozera (5%)

Methodology: Designed and detailed the FTIR (Fourier-Transform Infrared Spectroscopy) approach for adhesive characterization.

Investigation: Performed FTIR experiments and gathered spectral data.

Writing – Original Draft: Wrote the methods subsection for FTIR analysis and contributed to result interpretation.

9. Alejandro J. Muller (8%)

Supervision: Oversaw the thermal analyses and tack property investigations, offering high-level guidance and mentorship.

Writing – Review & Editing: Provided critical revisions, ensuring the scientific soundness and cohesion of the manuscript.

10. Savvas G. Hatzikiriakos (3%)

Supervision: Supervised the rheological part of the study, giving expert input on experimental design and data interpretation.

Writing – Review & Editing: Critically reviewed the manuscript for technical accuracy and overall coherence.

11. Anna Boczkowska (3%)

Supervision: Provided overarching project oversight, leadership in research planning, and external mentorship to the team.

All authors have read and approved the final manuscript. Each individual's contribution was essential for the completeness and quality of this research. We confirm that these roles and percentage allocations accurately reflect the work carried out by each contributor.

ORCID

Michał Misiak http://orcid.org/0000-0002-2892-418X
Paulina Latko-Durałek http://orcid.org/0000-0002-1568-5431
Maria Mercedes Fernandez http://orcid.org/0000-0002-7322-8001
Jorge L. Olmedo-Martínez http://orcid.org/0000-0002-9743-8492
Dorota Kołbuk http://orcid.org/0000-0001-9651-7087
Żaneta Górecka http://orcid.org/0000-0003-4782-6128
Amir Malmir http://orcid.org/0009-0000-5945-593X
Paulina Kozera http://orcid.org/0000-0002-4092-7746
Alejandro J. Müller http://orcid.org/0000-0001-7009-7715
Savvas G. Hatzikiriakos http://orcid.org/0000-0002-1456-7927
Anna Boczkowska http://orcid.org/0000-0002-3694-1342

References

[1] Kostyuk, A., N. Smirnova, S. Antonov, and S. Ilyin. 2021. Rheological and adhesion properties of hot-melt adhesives based on hydrocarbon resins and poly(ethylene-vinyl acetate). *Polym. Sci. Ser. A* 63:283–295. doi:10.1134/S0965545X21030081

[2] Pengelly, I., J. Groves, and C. Northage. 1998. An investigation into the composition of products evolved during heating of hot melt adhesives. *Ann. Occup. Hyg.* 42:37–44. doi:10.1016/s0003-4878(97)00045-8

[3] Sasikumar Kala, V., and R. Gadhave. 2020. Sustainable raw materials in hot melt adhesives: a review. *Open J. Polym. Chem.* 10:49–65.

[4] Viljanmaa, M., A. Södergård, and P. Törmälä. 2002. Lactic acid based polymers as hot melt adhesives for packaging applications. *Int. J. Adhes. Adhes.* 22:219–226. doi:10.1016/S0143-7496(01)00057-4

[5] Glawe, A., R. Reuscher, R. Koppe, and T. Kolbusch. 2003. Hot-melt application for functional compounds on technical textiles. *J. Ind. Text.* 33:85–92. doi:10.1177/152808303038587

[6] Blyberg, L., M. Lang, K. Lundstedt, M. Schander, E. Serrano, M. Silfverhielm, and C. Stålhandske. 2014. Glass, timber and adhesive joints – innovative load bearing building components. *Constr. Build. Mater.* 55:470–478. doi:10.1016/j.conbuildmat.2014.01.045

[7] Malysheva, G., and N. Bodrykh. 2011. Hot-melt adhesives. *Polym. Sci. Ser. D* 4:301–303. doi:10.1134/S1995421211040095

[8] Koricho, E. G., E. Verna, G. Belingardi, B. Martorana, and V. Brunella. 2016. Parametric study of hot-melt adhesive under accelerated ageing for automotive applications. *Int. J. Adhes. Adhes.* 68:169–181. doi:10.1016/j.ijadhadh.2016.03.006

[9] Hao, J., D. Wang, S. Li, X. He, J. Zhou, and F. Xue. 2017. The effect of conductive filler on the properties of electrically Conductive Adhesives (ECAs). In *2017 18th International Conference on Electronic Packaging Technology (ICEPT)*, pp. 803–808. Piscataway, NJ: IEEE. doi:10.1109/ICEPT.2017.8046567

[10] Latko-Durałek, P., R. Kozera, J. Macutkevič, K. Dydek, and A. Boczkowska. 2020. Relationship between viscosity, microstructure and electrical conductivity in copolyamide hot melt adhesives containing carbon nanotubes. *Materials* 13:4469. doi:10.3390/ma13204469

[11] Li, W., L. Bouzidi, and S. Narine. 2008. Current research and development status and prospect of hot-melt adhesives: a review. *Ind. Eng. Chem. Res.* 47:7524–7532. doi:10.1021/ie800189b

[12] Antonov, S., V. Ignatenko, T. Anokhina, S. Ilyin, A. Kostyuk, D. Bakhtin, V. Makarova, and A. Volkov. 2020. Phase separation of polymethylpentene solutions for producing microfiltration membranes. *Polym. Sci. Ser. A* 62:292–299. doi:10.1134/S0965545X20030098

[13] Ilyin, S., V. Melekhina, A. Kostyuk, and N. Smirnova. 2022. Hot-Melt and pressure-sensitive adhesives based on styrene-isoprene-styrene triblock copolymer, asphaltene/resin blend and naphthenic oil. *Polymers (Basel)* 14:4296. doi:10.3390/polym14204296

[14] Ignatenko, V. Y., A. V. Kostyuk, N. M. Smirnova, S. V. Antonov, and S. O. Ilyin. 2020. Asphaltenes as a tackifier for hot-melt adhesives based on the styrene-isoprene-styrene block copolymer. *Polym. Eng. Sci.* 60:2224–2234. doi:10.1002/pen.25465

[15] Ilyin, S. O., V. V. Makarova, M. Y. Polyakova, and V. G. Kulichikhin. 2020. Phase behavior and rheology of miscible and immiscible blends of linear and hyperbranched siloxane macromolecules. *Mater. Today Commun.* 22:100833. doi:10.1016/j.mtcomm.2019.100833

[16] Kalish, J. P., S. Ramalingam, H. Bao, D. Hall, O. Wamuo, S. L. Hsu, C. W. Paul, A. Eodice, and Y.-G. Low. 2015. An analysis of the role of wax in hot melt adhesives. *Int. J. Adhes. Adhes.* 60:63–68. doi:10.1016/j.ijadhadh.2015.03.008

[17] Kim, J., H. Kim, J. Lim, K. S. Cho, and K. Min. 2012. Thermal properties and adhesion strength of amorphous poly(α-olefins)/styrene–ethylene–butylene copolymer/terpene hot-melt adhesive. *J. Appl. Polym. Sci.* 124(6):4790–4798. doi:10.1002/app.35368

[18] Latko-Durałek, P., K. Dydek, P. Bolimowski, E. Golonko, P. Durałek, R. Kozera, and A. Boczkowska. 2018. Nonwoven fabrics with carbon nanotubes used as interleaves in CFRP. *IOP Conf. Ser: Mater. Sci. Eng.* 406:012033. doi:10.1088/1757-899X/406/1/012033

[19] Tian, J. L., Y. M. Cao, and X. Q. Zhou. 2011. Study on properties and preparation of thermoplastic polyurethane hot-melt adhesive. *Adv. Mater. Res.* 311-313:1071–1076. doi:10.4028/www.scientific.net/AMR.311-313.1071

[20] Hot Melt Adhesives Market Share & Trends Forecasts - 2032. *Glob. Mark. Insights Inc.* https://www.gminsights.com/industry-analysis/hot-melt-adhesives-market.

[21] Peng, X., S. Liu, Y. Huang, and L. Sang. 2020. Investigation of joining of continuous glass fibre reinforced polypropylene laminates via fusion bonding and hotmelt adhesive film. *Int. J. Adhes. Adhes.* 100:102615. doi:10.1016/j.ijadhadh.2020.102615

[22] Amini, G., and A. A. Gharehaghaji. 2018. Improving adhesion of electrospun nanofiber mats to supporting substrate by using adhesive bonding. *Int. J. Adhes. Adhes.* 86:40–44. doi:10.1016/j.ijadhadh.2018.08.005

[23] Chu, H.-H., W.-H. Huang, K. S. Chuang, and B.-H. Shen. 2020. Adhesion and viscoelastic property of poly(ethylene-co-vinyl acetate) based hot melt adhesives- effects of tackifier and wax. *Int. J. Adhes. Adhes.* 99:102586. doi:10.1016/j.ijadhadh.2020.102586

[24] Karakaya, N., M. Papila, and G. Özkoç. 2020. Effects of hot melt adhesives on the interfacial properties of overmolded hybrid structures of polyamide-6 on continuous carbon fiber/epoxy composites. *Compos. Part Appl. Sci. Manuf.* 139:106106. doi:10.1016/j.compositesa.2020.106106

[25] Sandoval, A. J., M. M. Fernández, M. V. Candal, M. Safari, A. Santamaria, and A. J. Müller. 2022. Rheology and tack properties of biodegradable isodimorphic poly(butylene succinate)-Ran-Poly(ε-caprolactone) random copolyesters and their potential use as adhesives. *Polymers (Basel)* 14:623. doi:10.3390/polym14030623

[26] Irska, I., S. Paszkiewicz, K. Goracy, A. Linares, T. A. Ezquerra, R. Jedrzejewski, Z. Roslaniec, and E. Piesowicz. 2020. Poly(butylene terephthalate)/polylactic acid based copolyesters and blends: miscibility-structure-property relationship. *eXPRESS Polym. Lett.* 14:26–47. doi:10.3144/expresspolymlett.2020.4

[27] Pereira, G., F. Darabas Rzatki, L. Mazzaferro, D. Forin, and G. Barra. 2016. Mechanical and thermo-physical properties of short glass fiber reinforced polybutylene terephthalate upon aging in lubricant/refrigerant mixture. *Mat. Res.* 19:1310–1318. doi:10.1590/1980-5373-mr-2016-0339

[28] Ślusarczyk, C., M. Sieradzka, J. Fabia, and R. Fryczkowski. 2020. Supermolecular structure of poly(butylene terephthalate) fibers formed with the addition of reduced graphene oxide. *Polymers. (Basel)* 12:1456. doi:10.3390/polym12071456

[29] Tomisawa, R., T. Ikaga, K. H. Kim, Y. Ohkoshi, K. Okada, H. Masunaga, T. Kanaya, M. Masuda, and Y. Maeda. 2017. Effect of melt spinning conditions on the fiber structure development of polyethylene tere-phthalate. *Polymer* 116:367–377. doi:10.1016/j.polymer.2016.12.077

[30] Davis, G. D., L. F. M. da Silva, A. Öchsner, and R. D. Adams. pp 2011. Surface treatments of selected materials. In *Handbook of Adhesion Technology*, pp. 147–177. Berlin, Heidelberg: Springer. doi:10.1007/978-3-642-01169-6_8

[31] O'Connor, A. E., and N. Willenbacher. 2004. The effect of molecular weight and temperature on tack properties of model polyisobutylenes. *Int. J. Adhes. Adhes.* 24:335–346. doi:10.1016/j.ijadhadh.2003.11.005

[32] Strobl, G. 2007. *The Physics of Polymers*. Berlin, Heidelberg: Springer. doi:10.1007/978-3-540-68411-4

[33] Fernández-Tena, A., R. A. Pérez-Camargo, O. Coulembier, L. Sangroniz, N. Aranburu, G. Guerrica-Echevarria, G. Liu, D. Wang, D. Cavallo, and A. J. Müller. 2023. Effect of molecular weight on the crystallization and melt memory of poly(ε-caprolactone) (PCL). *Macromolecules* 56:4602–4620. doi:10.1021/acs.macromol.3c00234

[34] Callies, X., C. Fonteneau, S. Pensec, L. Bouteiller, G. Ducouret, and C. Creton. 2016. Adhesion and non-linear rheology of adhesives with supramolecular crosslinking points. *Soft Matter* 12:7174–7185. doi:10.1039/c6sm01154c

[35] Lakrout, H., P. Sergot, and C. Creton. 1999. Direct observation of cavitation and fibrillation in a probe tack experiment on model acrylic pressure-sensitive-adhesives. *J. Adhes.* 69:307–359. doi:10.1080/00218469908017233

[36] Tordjeman, P., E. Papon, and J.-J. Villenave. 2000. Tack properties of pressure-sensitive adhesives. *J. Polym. Sci. B Polym. Phys.* 38:1201–1208. doi:10.1002/(SICI)1099-0488(20000501)38:9<1201::AID-POLB12>3.3.CO;2-R

[37] Deplace, F., C. Carelli, S. Mariot, H. Retsos, A. Chateauminois, K. Ouzineb, and C. Creton. 2009. Fine tuning the adhesive properties of a soft nanostructured adhesive with rheological measurements. *J. Adhes.* 85:18–54. doi:10.1080/00218460902727381

[38] Creton, C., and P. Fabre. 2021. Tack. In *Comprehensive Adhesion Science*, *Vol. II: The Mechanics of Adhesion, Rheology of Adhesives and Strength of Adhesive Bonds*, ed. D. A. Dillard. Amsterdam, The Netherlands: Elsevier.

[39] Lakrout, H., C. Creton, D. Ahn, and K. R. Shull. 2001. Influence of molecular features on the tackiness of acrylic polymer melts. *Macromolecules* 34:7448–7458. doi:10.1021/ma0020279

[40] Creton, C., and M. Ciccotti. 2016. Fracture and adhesion of soft materials: a review. *Rep. Prog. Phys.* 79:046601. doi:10.1088/0034-4885/79/4/046601

[41] Chiche, A., J. Dollhofer, and C. Creton. 2005. Cavity growth in soft adhesives. *Eur. Phys. J. E Soft Matter* 17:389–401. doi:10.1140/epje/i2004-10148-3

[42] Lindner, A., B. Lestriez, S. Mariot, C. Creton, T. Maevis, B. Lühmann, and R. Brummer. 2006. Adhesive and rheological properties of lightly crosslinked model acrylic networks. *J. Adhes.* 82:267–310. doi:10.1080/00218460600646594

[43] Akram, N., R. S. Gurney, M. Zuber, M. Ishaq, and J. L. Keddie. 2013. Influence of polyol molecular weight and type on the tack and peel properties of waterborne polyurethane pressure- S ensitive adhesives. *Macro React. Eng.* 7:493–503. doi:10.1002/mren.201300109

[44] Li, P.-R., Y.-H. Chen, and S.-P. Rwei. 2023. Effect of side group and crosslinking on the copolyesters as solvent-free pressure-sensitive adhesives. *Int. J. Adhes. Adhes.* 127:103494. doi:10.1016/j.ijadhadh.2023.103494